STUDY OF WAKE REGION OF A TYPICAL ISOLATED BUILDINGS. PART I: FLOW VISUALIZATION

Artur Burgo, arturburgo@gmail.com
Reginaldo Rosa Cotto de Paula, reginaldo@ifes.edu.br
Coordenadoria de Engenharia Sanitária e Ambiental, Ifes, Campus Vitória, Vitória, Brasil

Fernanda Capucho Cezana, fe.cezana@gmail.com
Coordenadoria de Matemática, Ifes, Campus Vitória, Vitória, Brasil

Bianca Hulle de Souza, bibihulle@hotmail.com
Coordenadoria de Mecânica, Ifes, Campus Vitória, Vitória, Brasil

Marcos Sebastião de Paula Gomes, mspgomes@mec.puc-rio.br
Departamento de Engenharia Mecânica, PUC-Rio, Rio de Janeiro, Brasil

Abstract. *In this work the wind tunnel experiments of wind flow around isolated buildings were performed in order to investigate the flow pattern and lengths of the reattachment points on the top and the near wake of the body. The experiments were conducted in a neutral atmospheric boundary layer wind tunnel by using cubic and rectangular prismatic buildings for comparisons of the flow patterns. For the oncoming flow, one building orientation relative to the incident wind with different velocities were considered. The flow visualization technique was used to study the effects of model scale building geometries on the wind field behavior. The results obtained by visualization experiments presented a generally similar patter in the vortex system, however with different dimensions of the flow region.*

Keywords: *building flow, wind tunnel experiments, flow visualization, atmospheric boundary layer.*

1. INTRODUCTION

In many practical applications, such as wind load (Ikhwan and Ruck, 2006), dispersion of air pollutants (Santos *et al*., 2009), natural ventilation system (Walker *et al*., 2011) and indoor pollution (Liu *et al*., 2010), it is essential to understanding the air flow patterns around buildings. Previous studies have been show that the field flow around an isolated building submerge in boundary layer is characterized by a complex tree-dimensional structures (Becker *et al*., 2002). This flow is characterized by five main regions: incident turbulent flow, near wake flow, turbulence wake, horse-vortex system and reattachment of the flow in the building faces (Hosker, 1981; Santos, 2000). The interaction of the flow-building system depends on a larger number of parameters, such as obstacle geometry, free-stream turbulence and approaching boundary layer flow.

Many studies of the wind flow past around an isolated building have been conducted considering field and wind tunnel, towing-tank experiments and numerical simulations (Martinuzzi and Tropea, 1993; Dijk and Lange, 2007) . It is particularly of great interest to analyze the structure and dynamics of near wake region.

Huber *et al*. (1991) used video images of smoke in a wind tunnel study of dispersion in the near wake of a rectangular-shaped block model building in a neutral stratified boundary layer. The video image technique has been shown to have a great potential as an easily electronic medium for studying the dispersion of smoke around bodies.

Choiniere and Munroe (1994) realized wind tunnel experiments using a 1:20 scale model of a naturally ventilated barn with gable roof and sloped ceilings. The aim was to visualize three-dimensional airflow patterns inside the model for different incident wind angles and determined the effect on airflow patterns by sidewall door opening angle; ridge opening width, end wall windows, the addition of a cross-wall at midlength and sidewall doors open on the leeward side only. The authors used smoke to visualize the airflow structure in single-side situations with different wind directions. Each building configuration was tested with the incident wind at 0, 30, 60 and 90 degrees. The results showed that the optimum ventilation patters were observed for wind perpendicular to the building length. In case of parallel winds, the addition of windows in the end wall reduced the size of zones of slow smoke dispersion inside the scale model.

Yang and Hwang (2000) performed a numerical simulation of laminar horseshoe vortex system around cubic obstacle in a channel for Reynolds number varying form 5 to 1500. They found that unsteady horseshoe vortex systems were observed in the entrance region of the channel for Re > 20, downstream of the obstacle a three-dimensional wake was formed.

Becker *et al*. (2002) carried out wind tunnel experiments to investigate the structure of the flow field around three-dimensional obstacles of different aspect rations. The studies of the flow were performed using different kinds of flow visualization techniques and laser Doppler anemometry (LDA). The results showed the dependence of the field flow around the obstacle on its aspect ratio, the incident wind attack angle, the Reynolds number and the type of boundary layer.

Cezana (2007) realized numerical simulations to investigate the flow and dispersion of pollutants in the vicinity of single obstacles. Numerical simulations with the use of the κ-ε standard and the Reynolds Stress Model were performed considering the dispersion in neutral, stable and unstable atmospheric condition over flat terrain with an isolated cubic building. The results obtained for the numerical simulations under different atmospheric stability conditions showed that this parameter strongly affects the flow and dispersion around the building.

In this study, an investigation of the wind-flow structure around buildings with different aspect ratio was examined in wind tunnel experiments. For flow visualization were used the smoke injection technique and video camera in order to identified the flow patterns around an isolated building. Measurements with Pitot probe were carried out to estimate the near wake length.

2. MATERIAL AND METHODS

The flow considered in this work was investigated in open return wind tunnel with test section of 2.0 m × 0.5 m × 0.5 m of the Energy Laboratory of Ifes, Vitoria, Brazil. Wood spires (0.379 m) and roughness elements (cubical wooden blocks of 0.015 m) were installed upwind of test area of the wind tunnel in order to generate a neutral atmospheric boundary layer (Irwin, 1981). The mean streamwise velocity has the following power la profile:

$$\frac{U(z)}{U_\delta} = \left(\frac{y}{\delta}\right)^p \tag{1}$$

where δ = 0.30 m is the atmospheric boundary layer thickness. The velocity profile was fitted with $p = 0.20$, which corresponds to the velocity profile over flat terrain with low buildings (Blessman, 1988).

Three models scale building (1/100) used in wind tunnel experiments were a cube ($W/H = 1.0$ m), and two rectangular prismatic with different aspect ratios ($L/H = 2.0$ and $L/H = 0.5$), where H is the building height and L is the length of side face of the obstacle. Figure 1 shows the sketch of the flow field analyzed in this study. Fluid of the smoke machine (LASER DJ 1500 W) and injections methods were utilized for the flow visualization. Video recordings were made with digital camera Fujifilm HS 10 with speed of the 240 fps (frames per second).
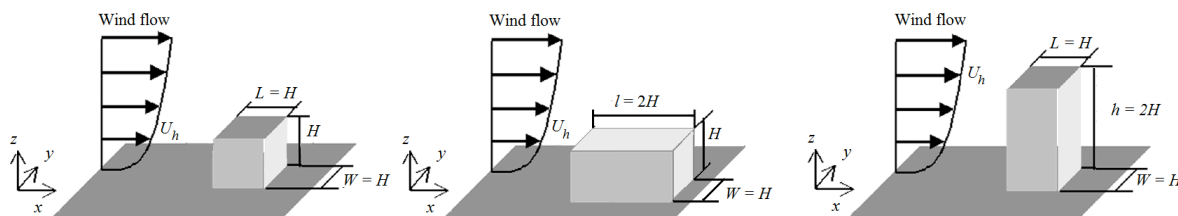

Figure 1. Sketches of the flow fields analyzed in this study.

In this work the Reynolds numbers were based on building height H and wind velocity at the building height, U_h. In addition were used air density of 1.185 kg/m^3 and air viscosity of 1.82×10^{-5} kg / m^2.s. Table 1 shows the measurements of the mean wind velocity at building height and correspondent Reynolds number.

Table 1. Results of measurements of the mean wind velocity at building height and Re numbers for tree buildings analyzed.

L/H = 1.0		L/H = 2.0		L/H = 0.5	
U_h (m/s)	Re	U_h (m/s)	Re	U_h (m/s)	Re
0.273	1.8×10^3	0.273	1.8×10^3	0.325	4.2×10^3
0.499	3.2×10^3	0.499	3.2×10^3	0.677	8.8×10^3
1.093	7.1×10^3	1.093	7.1×10^3	1.364	1.7×10^4
2.304	1.5×10^4	2.304	1.5×10^4	2.703	3.5×10^4

3. RESULTS

Figures 2 to 5 show the results of flow visualization in frontal face of cubic building ($L/H = 1.0$) at Reynolds numbers in the range of 1.8×10^3 to 1.5×10^4. Qualitatively various features of the flow were correctly captured by recording the images. In frontal face of the building, the fluid flow toward the ground and return in the opposite

direction to the main flow. This interaction between the incident flow and reverse flow generated the standing vortex near the ground a as show Figs. 2 to 5. It is evident that the results obtained by flow visualization were able to show the separation and the reattachment point of the boundary layer on the roof of the building as showed Figs. 2, 3, 4 and 5.
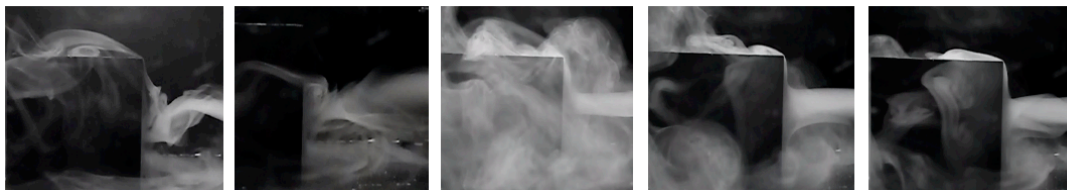

Figure 2. Side view of the incident flow around cubic building (L/H = 1.0) at Re = 1.8 $\times 10^3$.

Figure 3. Side view of the incident flow around cubic building (L/H = 1.0) at Re = 3.2 $\times 10^3$.

Figure 4. Side view of the incident flow around cubic building (L/H = 1.0) at Re = 7.1 $\times 10^3$.
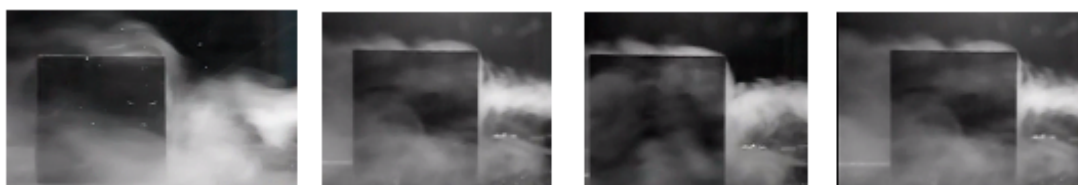

Figure 5. Side view of the incident flow around cubic building (L/H = 1.0) at Re = 1.5 $\times 10^4$.

Figures 6 and 7 show the flow structure in the near wake region behind of the cubic building at low Reynolds. The simulated boundary layer caused a recirculation zone behind the building, which shows similar pattern for different Reynolds number. This region was characterized by intense circulation motion, low flow velocities and complex three-dimensional structures.
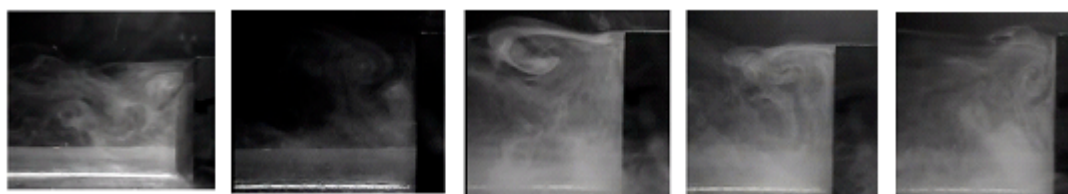

Figure 6. Side view of the flow in near wake around cubic building (L/H = 1.0) at Re = 1.8 $\times 10^3$.

Figure 7. Side view of the flow in near wake around cubic building (L/H = 1.0) at Re = 3.2 $\times 10^3$.

Figures 8 and 9 show the flow structure in the near wake region behind of the cubic building at high Reynolds numbers. The simulated boundary layer caused a recirculation zone behind the building, which shows similar pattern for different Reynolds number. However, in the captured images was not as clearly as it was visualized in loco.

Figure 8. Side view of the flow in near wake around cubic building ($L/H = 1.0$) at Re = 7.1×10^3.

Figure 9. Side view of the flow in near wake around cubic building ($L/H = 1.0$) at Re = 1.5×10^4.

Figures 10 to 13 showed the results of flow visualization in frontal face of the rectangular prismatic building ($L/H = 2.0$) at Reynolds numbers in the range of 1.8×10^3 to 1.5×10^4. Comparing pictures for the rectangular prismatic obstacle, was observed out that there were no fundamental changes in the vortex structure with the increases of the Reynolds number.

Figure 10. Side view of the incident flow rectangular prismatic building ($L/H = 2.0$) at Re = 1.8×10^3.
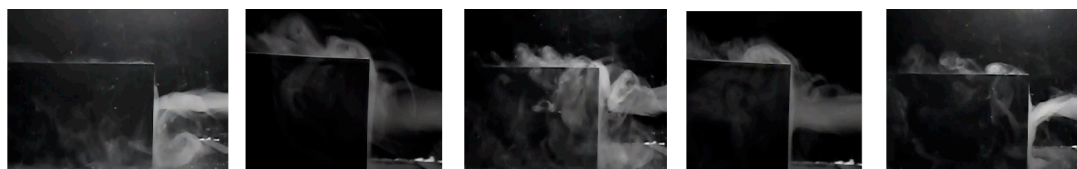

Figure 11. Side view of the incident flow around rectangular prismatic building ($L/H = 2.0$) at Re = 3.2×10^3.

Figure 12. Side view of the incident flow around rectangular prismatic building ($L/H = 2.0$) at Re = 7.1×10^3.

Figure 13. Side view of the incident flow around rectangular prismatic building ($L/H = 2.0$) at Re = 1.5×10^4.

Figures 14 to 15 present the results of the flow visualization in the near wake behind the rectangular prismatic building. The last picture in the Fig. 14 shows the horseshoe vortex system due to interaction between the incident flow and reverse flow that causes a lateral motion and generates the horseshoe vortex.
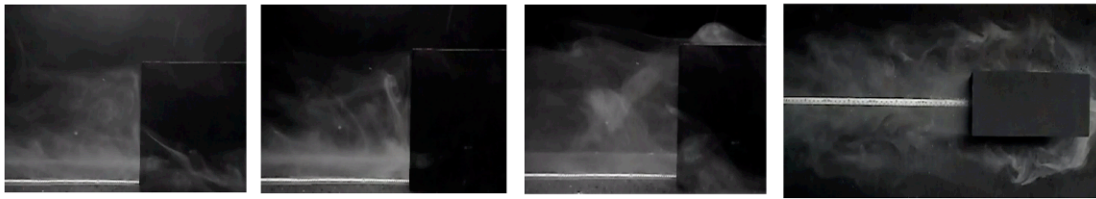
Figure 14. View of the flow in the wake near around rectangular prismatic building ($L/H = 2.0$) at Re = 1.8 ×10^3.

Figure 15. Side view of the near wake flow around rectangular prismatic building ($L/H = 2.0$) at Re = 3.2 ×10^3.

Figures 16 to 19 show the results of flow visualization around rectangular prismatic building ($L/H = 0.5$) at Reynolds numbers in the range of 4.2 × 10^3 - 3.5 × 10^4. Comparing cubic and rectangular buildings, it was observed that there was no fundamental change in the vortex structure. In the last pictures of the Figs. 16 to 19 it were possible to observe the horseshoe vortex formation system due to interaction between incident an reverse flow in frontal face of the building.
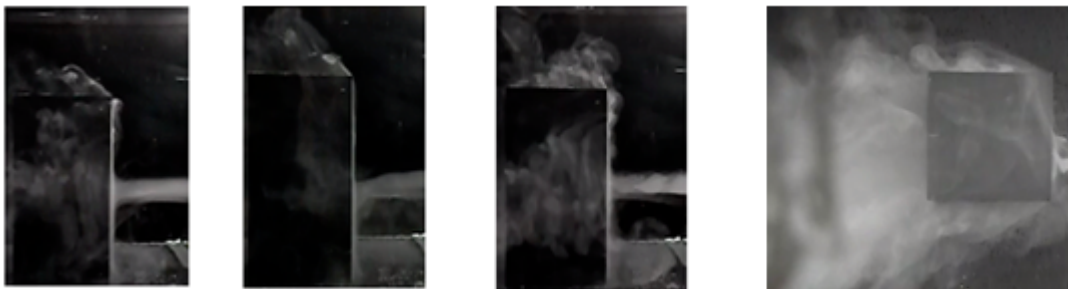

Figure 16. View of the flow in the vicinity of the rectangular prismatic building ($L/H = 0.5$) at Re = 4.2×10^3.

Figure 17. View of the flow in the vicinity of the rectangular prismatic building ($L/H = 0.5$) at Re = 8.8 × 10^3

Figure 18. View of the flow in the vicinity of the rectangular prismatic building ($L/H = 0.5$) at Re = 1.7 × 10^4.
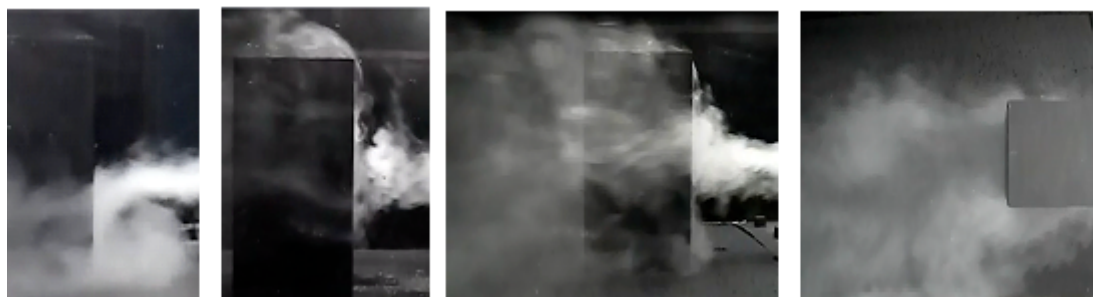
Figure 19. View of the flow in the vicinity of the rectangular prismatic building ($L/H = 0.5$) at Re $= 3.5 \times 10^4$.

Table 2 shows the localization of normalized reattachment point (x_R/H) on the roof of buildings at different Reynolds numbers. The results showed that in the roof the ratio x_R/H decreases with increasing Reynolds number. It was also observed that the ratio x_R/H decreases with increasing of height of the building and increases with increasing of length.

Table 2. Localization of reattachment point in the roof of buildings at different Reynolds numbers. This point was normalized by building height (x_R / H).

L/H	$Re_H = 1.8 \times 10^3$	$Re_H = 3.2 \times 10^3$	$Re_H = 7.1 \times 10^3$	$Re_H = 1.5 \times 10^4$
1.0	0.60	0.41	0.33	0.24
2.0	0.68	0.53	0.51	0.45
	$Re_H = 4.2 \times 10^3$	$Re_H = 8.8 \times 10^3$	$Re_H = 1.7 \times 10^4$	$Re_H = 3.5 \times 10^4$
0.5	0.45	0.36	0.28	0.26

Table 3 presents the localization of reattachment lengths in the near wake of building at different Reynolds number normalized by building height (x_w/H). The results showed that throughout the separation bubble, the ratio x_w/H increases with increasing Reynolds number. In addition, it was observed that Reynolds number increases with increasing the length and height of the building.

Table 3. Localization of reattachment point in the wake region of buildings at different Reynolds numbers. This point was normalized by building height (x_w / H).

L/H	$Re_H = 1.8 \times 10^3$	$Re_H = 3.2 \times 10^3$	$Re_H = 7.1 \times 10^3$	$Re_H = 1.5 \times 10^4$
1.0	0.73	0.92	0.94	1.08
2.0	0.83	0.93	0.99	1.22
	$Re_H = 4.2 \times 10^3$	$Re_H = 8.8 \times 10^3$	$Re_H = 1.7 \times 10^4$	$Re_H = 3.5 \times 10^4$
0.5	0.94	1.01	0.98	1.00

Table 4 shows the comparison of experimental reattachment lengths on the roof (x_R/H) and behind cube (x_w/H) from different works. The length of the reattachment on the roof was comparable with those found by Lim *et al*. (2009) for the same range of Reynolds number. In the near wake region the length of the reattachment was comparable with the result found by Murakini *et al*., (1990).

Table 4. Comparison of experimental reattachment on the roof and behind cube from different works.

x_R/H	Re_H	Authors	x_W/H	Re_H	Authors	
0.24	1.5×10^4	Present work	1.08	1.5×10^4	Present work	
0.20	2.0×10^4	Lim et al. (2009)	1.2	7×10^4	Murakani et al. (1990)	
0.64	6.4×10^4	Li and Meroney (1983)	1.33	6.4×10^4	Li and Meroney (1983)	
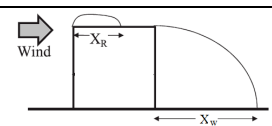
4. CONCLUSIONS

The present work described the investigation on the flow in the vicinity of cubic and rectangular prismatic obstacles immersed on a wind tunnel atmospheric boundary layer. The flow structure and the vortex system were studied under a variety of velocities of oncoming flow conditions and aspect ratio using flow visualization with the smoke injection technique. The results of the recorded images were able to capture the standing vortex in front of the obstacle, the horseshoe vortex system, the roof vortex on top of the obstacle and the near wake vortex system behind the obstacle. Comparing pictures for different boundary layer between the cubic and rectangular buildings, it was observed out that

there were no fundamental changes in the vortex structure. However, were observed a dependence of the reattachment length on the roof and the near wake, respectively x_R and x_w with the Reynolds number. These results suggested that flow around building presented a similar pattern in the vortex system, however with different dimensions of the flow region.

5. REFERENCES

Becker, S., Lienhart, H. and Durst, F., 2002. "Flow around three-dimensional obstacles in boundary layers." Journal of Wind Engineering and Industrial Aerodynamics", Vol. 90, pp. 265-279.

Blessmann, J., 1995. "O vento na Engenharia Estrutural". Editora Universidade, Universidade Federal do Rio Grande do Sul.

Cezana, F.C., 2007. Simulação numérica da dispersão de poluentes ao redor de um obstáculo isolado sob diferentes condições de estabilidade. Master thesis, Universidade Federal do Espírito Santo, Vitória, Brazil.

Choiniere, Y. and Munroe, J.A., 1994. "A wind-tunnel study of wind direction effects on air-flow patterns in naturally ventilated swine buildings", Canadian Agricultural Engineering, Vol. 36, pp. 93-101.

Ikhwan, M. and Ruck, B. 2006. "Flow and pressure field characteristics around pyramidal buildings." Journal of Wind Engineering and Industrial Aerodynamics, Vol. 94, pp. 745-765.

Liu, X.P., Niu, J.L., Kwok, K.C.S., Wang, J.H. and Li, B.Z., 2010. "Investigation of indoor air pollutant dispersion and cross-contamination around a typical high-rise residential building: wind tunnel tests." Building and Environment, Vol. 45, pp. 1769-1778.

Li, W. and Meroney, R.N., 1983a. "Gas Dispersion near a cubical model building, Part I, concentration measurements. Journal of Wind Engineering and Industrial Aerodynamics", Vol. 12, pp. 15-33.

Lim, C.H., Thomas, T.G. and Castro, I.P., 2009. "Flow Around a Cube in a Turbulent Boundary Layer: LES and Experiment." Journal of Wind Engineering and Industrial Aerodynamics, Vol. 97, pp. 96-109.

Martinuzzi, R. and Tropea, C., 1993. "The Flow Around Surface-Mounted, Prismatic Obstacles Placed in a Fully Developed Channel Flow." Journal of Fluids Engineering, Vol. 115, pp. 85-93.

Murakami S., Mochida A. and Yoshihiko H., 1990. "Examining the k-e Model by Means of a Wind Tunnel Test and Large Eddy Simulation of the Turbulence Structure Around a Cube." Journal of Wind Engineering and Industrial Aerodynamics, Vol. 35, pp. 87-100.

Santos, J.M., Reis, N.C., Goulart, E.V. and Mavroidis, I., 2009. "Numerical simulation of flow and dispersion around an isolated cubical building: The effect of the atmospheric stratification." Atmospheric Environment, Vol. 43, pp. 5484–5492.

Huber, A.H., Arya, S.P., Rajala, S.A. and Borek, J.W., 1991. "Preliminary Studies of Video Images of Smoke Dispersion in the Near Wake of a Model Building". Atmospheric Environment, Vol. 25A, pp. 1199-1209.

Walker, C., Tan, G. and Glicksman, L., 2011. "Reduced-scale building model and numerical investigations to buoyancy-driven natural ventilation." Energy and Buildings, Vol. 43, pp. 2404-2412.

Dijk, A. van and Lange, H.C., 2007. "Compressible laminar flow around a wall-mounted cubic obstacle." Computers & Fluids, Vol. 36, pp. 949–960.

6. RESPONSIBILITY NOTICE

The authors are the only responsible for the printed material included in this paper.